

Article

Effect of Ta₂O₅ and Nb₂O₅ Dopants on the Stable Dielectric Properties of BaTiO₃–(Bi_{0.5}Na_{0.5})TiO₃-Based Materials

Sea-Fue Wang ^{†,*}, Yung-Fu Hsu, Yu-Wen Hung and Yi-Xin Liu

Department of Materials and Mineral Resources Engineering, National Taipei University of Technology, Taipei 106, Taiwan; E-Mails: yfhsu@ntut.edu.tw (Y.-F.H.); lovemyky@gmail.com (Y.-W.H.); evie19831123@gmail.com (Y.-X.L.)

[†] Current Address: Department of Materials and Mineral Resources Engineering, National Taipei University of Technology, 1, Sec. 3, Chung-Hsiao E. Rd., Taipei 106, Taiwan.

* Author to whom correspondence should be addressed; E-Mail: sfwang@ntut.edu.tw; Tel.: +886-2-2771-2171 (ext. 2735).

Academic Editor: Sheng-Yuan Chu

Received: 4 September 2015 / Accepted: 2 November 2015 / Published: 16 November 2015

Abstract: In this study, BaTiO₃–(Bi_{0.5}Na_{0.5})TiO₃ ceramics with various amounts of Ta₂O₅ dopant were investigated for their ability to enhance high-temperature stability to meet X9R specifications. The results were compared to those for ceramics with the common Nb₂O₅ additive. The best composition appeared to be 0.9BaTiO₃–0.1(Bi_{0.5}Na_{0.5})TiO₃ with 2 mol% Ta₂O₅ dopant sintered at 1215 °C, which had a dielectric constant of 1386, a tanδ value of 1.8%, temperature coefficients of capacitance (TCCs) of –1.3% and 1.2%, and electrical resistivities of 2.8 × 10¹² and 1.5 × 10¹⁰ Ω·cm at 25 °C and 200 °C, respectively. Its microstructure consisted of fine equiaxed grains with a perovskite structure and an average grain size of 0.46 μm and some rod-like grains of second-phase Ba₆Ti₁₇O₄₀ with a size of approximately 3.2 μm. The Ta₂O₅ dopant caused a reduction in the grain size and a slight increase in trapped pores. The temperature dependence of the dielectric constant flattened and the Curie point was dramatically suppressed with the addition of Ta₂O₅ dopant, leading to smooth dielectric temperature characteristics over a relatively broad temperature range. The X9R formulations and their dielectric properties were highly repeatable in this study.

Keywords: dielectric properties; X9R; formulation; microstructure

1. Introduction

Multilayer ceramic capacitors (MLCCs) are crucial electronic components used in virtually every area of electronics, and the number and variety of their applications have steadily grown. During the past decade, MLCC manufacturers have been driven to accelerate progress in miniaturization, enhancement of volumetric efficiency, reinforcement of stability and reliability against environment, and cost reduction, none of which can be achieved without an improvement in materials formulation and processing technology. The compositions of most ceramic capacitors are based on ferroelectric barium titanate (BaTiO_3) materials. BaTiO_3 can be either chemically or physically modified to exhibit the required temperature-stable dielectric behavior [1].

MLCCs used in automobile electronic parts, such as anti-lock brake systems, engine electronic control units, crank angle sensors, and programmed fuel injections, are exposed to high-temperature working conditions of greater than approximately 130 °C in the engine room of an automobile. MLCCs with X8R specifications (X8R: -55 °C to 150 °C, $\Delta C/C_{25\text{ °C}} \leq \pm 15\%$) were developed to satisfy this requirement. Because of the dramatic variation in permittivity of BaTiO_3 ceramics above the Curie temperature ($T_c \approx 125\text{ °C}$), the X8R formulation makes use of the core-shell structure to retain the temperature-stable characteristic by adding rare earth elements with a smaller ionic radius, such as Tm, Yb, Lu, Sc, Er, and Y, to shift the T_c to higher temperatures [2–4]. Nevertheless, for aerospace, oil drilling, and various other applications, MLCCs in electronic devices must withstand even harsher working environments, typified by temperatures higher than 150 °C. Accordingly, Yuan *et al.* and a few other researchers have recently started to work on the development of dielectric formulations capable of satisfying X9R specifications (-55 °C to 200 °C, $\Delta C/C_{25\text{ °C}} \leq \pm 15\%$) [5–11]. The utilization of an effective Curie-point shifter, such as $(\text{Bi}_{0.5}\text{Na}_{0.5})\text{TiO}_3$ or PbTiO_3 , to increase the T_c point along with the formation of the core-shell structure was found to be an effective method for obtaining high-temperature stability [12–16]. Dielectric formulations, including BaTiO_3 -based compositions, such as BaTiO_3 - $(\text{Bi}_{0.5}\text{Na}_{0.5})\text{TiO}_3$ [5,7,8,14,17–19], BaTiO_3 - $\text{Bi}(\text{Zn}_{0.5}\text{Ti}_{0.5})\text{O}_3$ [16,20], and BaTiO_3 - $\text{Pb}(\text{Ti}_{0.55}\text{Sn}_{0.45})\text{O}_3$ [10] systems, and $(\text{Bi}_{0.5}\text{Na}_{0.5})\text{TiO}_3$ -based compositions, such as $(\text{Bi}_{0.5}\text{Na}_{0.5})\text{TiO}_3$ - BaTiO_3 - CaTiO_3 [6,9,21] systems, have been developed recently to meet the temperature coefficient of capacitance (TCC) requirements of the X9R specifications. Another approach was a multi-phase composite consisting of a high- T_c material and a low- T_c material. For instance, new X9R dielectrics based on the BaTiO_3 - LiTaO_3 compositions reported by Wang *et al.* can be sintered in a reducing atmosphere and are compatible with the base metal electrode (BME) process [22].

In the BaTiO_3 - $(\text{Bi}_{0.5}\text{Na}_{0.5})\text{TiO}_3$ system, $(\text{Bi}_{0.5}\text{Na}_{0.5})\text{TiO}_3$ shows strong ferroelectricity at room temperature, undergoes a phase transition with a broad dielectric maximum approximately close to 320 °C [8], and is considered as an ideal material to shift the Curie temperature of BaTiO_3 above 150 °C [15]. The distortion and deformation of BaTiO_3 structure induced by the substitution of Na^+ and Bi^{3+} into Ba sites by $(\text{Bi}_{0.5}\text{Na}_{0.5})\text{TiO}_3$ addition improves the stable temperature characteristics of the dielectric properties of BaTiO_3 . With the addition of Co_3O_4 and Nb_2O_5 , the stable dielectric properties of BaTiO_3 - $(\text{Bi}_{0.5}\text{Na}_{0.5})\text{TiO}_3$ were tailored to meet the X9R specification by adjusting the core-shell structure [14,15]. It was also shown in the literature that the dielectric properties of BaTiO_3 or bismuth-based compounds can be significantly enhanced with the addition of Ta_2O_5 , through tailoring the microstructure, improving densification, and shifting Curie temperature [23,24]. In this

study, BaTiO₃–(Bi_{0.5}Na_{0.5})TiO₃ dielectric ceramics incorporating various amounts of Ta₂O₅ additive were investigated to enhance their high temperature stability to meet the X9R specifications. The effect of the Ta₂O₅ additive on the densification, crystalline phase, microstructure development, and dielectric properties of BaTiO₃–(Bi_{0.5}Na_{0.5})TiO₃ ceramics compared to those of the common Nb₂O₅ additive under the same processing conditions were investigated and are discussed below.

2. Experimental Procedure

Dielectric powders of $(1 - x)\text{BaTiO}_3 - x(\text{Bi}_{0.5}\text{Na}_{0.5})\text{TiO}_3$ ceramics with various amounts of Ta₂O₅ and Nb₂O₅ were prepared using the solid-state reaction technique. Highly pure (>99.9% purity) BaTiO₃ (Ferro, reagent grade), Bi₂O₃ (SHOWA, reagent grade), Na₂CO₃ (SHOWA, reagent grade), TiO₂ (SHOWA, reagent grade), Ta₂O₅ (Alfa, reagent grade), and Nb₂O₅ (Alfa, reagent grade) were used as raw materials. The host material (Bi_{0.5}Na_{0.5})TiO₃ was prepared by mixing appropriate amounts of Bi₂O₃, Na₂CO₃, and TiO₂ and calcining them at 800 °C for 12 h, and the phase was identified using X-ray diffraction (XRD, Rigaku DMX-2200, Rigaku, Tokyo, Japan). Formulations based on compositions of $(1 - x)\text{BaTiO}_3 - x(\text{Bi}_{0.5}\text{Na}_{0.5})\text{TiO}_3$ ($x = 0.05, 0.1, \text{ and } 0.2$) with various amounts of Ta₂O₅ and Nb₂O₅ (0, 1.0, 1.5, and 2.0 mol%) were mixed and milled in methyl alcohol solution using polyethylene jars and zirconia balls for 24 h and then dried at 80 °C in an oven overnight. The mixed powders were added to 4 wt% of a 15 wt% Polyvinyl Alcohol (PVA) solution and were pressed into disc-shaped compacts under a uniaxial pressure of 120 MPa. The samples were then heat treated at 550 °C for 4 h to eliminate the PVA, followed by sintering at 1200 °C to 1245 °C. The heating and cooling rates were controlled at 5 °C/min for all samples, and the dwell time was set to 2 h.

The apparent density of the sintered ceramics was measured on five samples for each composition using the Archimedes method with de-ionized water. Phase identification on the polished surfaces of the sintered bulk ceramics was performed using X-ray diffraction (XRD, Siemens D5000, Karlsruhe, Germany). The microstructures of the sintered samples were examined with scanning electron microscopy (SEM, JEOL 6500F, Tokyo, Japan) and energy-dispersive spectroscopy (EDS). The average grain sizes of the sintered samples were determined using the linear intercept, which was calculated as the mean value of the measurement diagonals of about 200 grains. The dielectric properties of the sintered samples were measured as a function of temperature using an automatic measurement system incorporating a Delta Design Environmental Chamber with an LCR meter (HP 4284A, Santa Clara, CA, USA) at a frequency of 1 kHz. Before measurement, electrodes were fabricated on the disc samples using silver paste applied on opposing surfaces and fired at 750 °C. The measurements were performed during heating cycles from –55 °C to 130 °C at a rate of 2 °C/min with an accuracy of 0.1 °C. An alternating voltage of 1 V was applied. The electrical resistivity of the bulk ceramics was determined by a high resistance meter (HP 4339B, Santa Clara, CA, USA) at 25 and 200 °C at a DC voltage of 500 V. The measurements of dielectric properties and electrical resistivity were performed on at least three samples in each case, with an accuracy of ±3%.

3. Results and Discussion

To determine the best composition of the host $(1 - x)\text{BaTiO}_3 - x(\text{Bi}_{0.5}\text{Na}_{0.5})\text{TiO}_3$ ceramic, formulations with an x value of 0.05, 0.1, or 0.2 were prepared and characterized. While the sintering

temperature of BaTiO₃ is typically above 1300 °C, the addition of (Bi_{0.5}Na_{0.5})TiO₃ significantly reduced the sintering temperature to 1230 °C for an x value of 0.05 and to 1215 °C for x values of 0.1 and 0.2, which was caused by the formation of the liquid phase [14,25]. XRD results indicated the presence of the tetragonal BaTiO₃ perovskite phase (tetragonal, P4/mmm; JCPDF 75-0462) with trace amounts of second-phase Ba₆Ti₁₇O₄₀ (monoclinic, C2/c; JCPDF 77-1566), which increased with the (Bi_{0.5}Na_{0.5})TiO₃ content. This observation is in accord with those reported in the literature [25,26]. In addition, the peaks corresponding to BaTiO₃ in the XRD patterns shifted to lower angles due to the incorporation of the smaller ions Na⁺ (VI; 1.02 Å) and Bi³⁺ (VI; 1.03 Å) in the Ba²⁺ (VI; 1.35 Å) sites. The lattice constants calculated from XRD patterns appeared to be $a = 3.991$ Å and $c = 4.025$ Å. The dielectric properties of the $(1 - x)\text{BaTiO}_3 - x(\text{Bi}_{0.5}\text{Na}_{0.5})\text{TiO}_3$ at the maximum density, measured at a frequency of 1 KHz, are listed in Table 1. The Curie point of the $(1 - x)\text{BaTiO}_3 - x(\text{Bi}_{0.5}\text{Na}_{0.5})\text{TiO}_3$ increased with the (Bi_{0.5}Na_{0.5})TiO₃ content and was 145 °C, 170 °C, and >200 °C for x values of 0.05, 0.1, and 0.2, respectively. This increase occurred because Bi–O bonds are weaker than Ba–O bonds, the substitution of Bi³⁺ into Ba sites leads to strengthened Ti–O bonds, and more energy is needed to maintain the balance of Ti⁴⁺ displacement in the TiO₆ octahedrons; thus, T_c increased [14,15,19]. The dielectric constant of $(1 - x)\text{BaTiO}_3 - x(\text{Bi}_{0.5}\text{Na}_{0.5})\text{TiO}_3$ at 25 °C decreased from 2066 to 677 while the $\tan\delta$ value increased from 2.9% to 3.5% as the x value increased from 0.05 to 0.2. The TCC at the cold end (–55 °C) decreased slightly from –20.8% to –24.6%, whereas the TCC at the hot end (200 °C) significantly increased from 27.0% to 641.0%, which was simply due to the increase in T_c . Because a high dielectric constant, a low $\tan\delta$ value, and a stable TCC are needed for X9R materials, the 0.9BaTiO₃–0.1(Bi_{0.5}Na_{0.5})TiO₃ ceramic was selected as the host material to incorporate the Ta₂O₅ and Nb₂O₅ additives in this study.

Figure 1a shows the sintered densities of 0.9BaTiO₃–0.1(Bi_{0.5}Na_{0.5})TiO₃ ceramics with 1.0%, 1.5%, and 2.0% Ta₂O₅ sintered at different temperatures. In all cases, the sintered density increased the sintering temperature, and the maximum densification was reached at 1215 °C. With further increases in sintering temperature, the sintered density gradually declined because of the trapped porosities associated with the fast grain growth and partly the evaporation of the volatile species such as bismuth and sodium. The weight losses of the Ta₂O₅-doped 0.9BaTiO₃–0.1(Bi_{0.5}Na_{0.5})TiO₃ ceramics during sintering were found to be less than 1.5 wt% through careful monitoring in this study, suggesting that the deviations of the sintered compositions from the nominal composition were only slight. The sintered density of the ceramics decreased slightly with an increase in Ta₂O₅ content, though Ta has a high molecular weight than the substituted Ti. For instance, the maximum densities of 0.9BaTiO₃–0.1(Bi_{0.5}Na_{0.5})TiO₃ ceramics with 1.0%, 1.5%, and 2.0% Ta₂O₅ were 5.82, 5.81, and 5.79 g/cm³, respectively. The results imply that the addition of Ta₂O₅ inhibits the sintering of the host material. As shown in Figure 1b, the sintered densities of 0.9BaTiO₃–0.1(Bi_{0.5}Na_{0.5})TiO₃ ceramics with 1.0%, 1.5%, and 2.0% Nb₂O₅ dopant showed a trend similar to those with added Ta₂O₅. Apparently, both Ta₂O₅ and Nb₂O₅ additives slightly obstructed the densification of the 0.9BaTiO₃–0.1(Bi_{0.5}Na_{0.5})TiO₃ ceramic.

Table 1. Dielectric properties of $(1 - x)\text{BaTiO}_3 - x(\text{Bi}_{0.5}\text{Na}_{0.5})\text{TiO}_3$ ceramics at their maximum sintered densities.

Starting Composition	Sintering Condition (°C/h)	Sintered Density (g/cm ³)	T _c (°C)	K (25 °C)	tanδ (25 °C)	TCC		Resistivity * (Ω·cm)	
						-55 °C	200 °C	25 °C	200 °C
0.95BaTiO ₃ -0.05(Bi _{0.5} Na _{0.5})TiO ₃	1230/2	5.78	145	2066	2.9%	-20.8	27.0	4.4 × 10 ¹²	9.2 × 10 ¹⁰
0.9BaTiO ₃ -0.1(Bi _{0.5} Na _{0.5})TiO ₃	1215/2	5.78	170	1044	3.4%	-26.2	202.0	7.2 × 10 ¹²	1.4 × 10 ¹¹
0.8BaTiO ₃ -0.2(Bi _{0.5} Na _{0.5})TiO ₃	1215/2	5.82	>200	677	3.5%	-24.6	641.0	1.9 × 10 ¹³	5.1 × 10 ¹⁰

* Resistivity of the samples was measured at a DC voltage of 500 V.

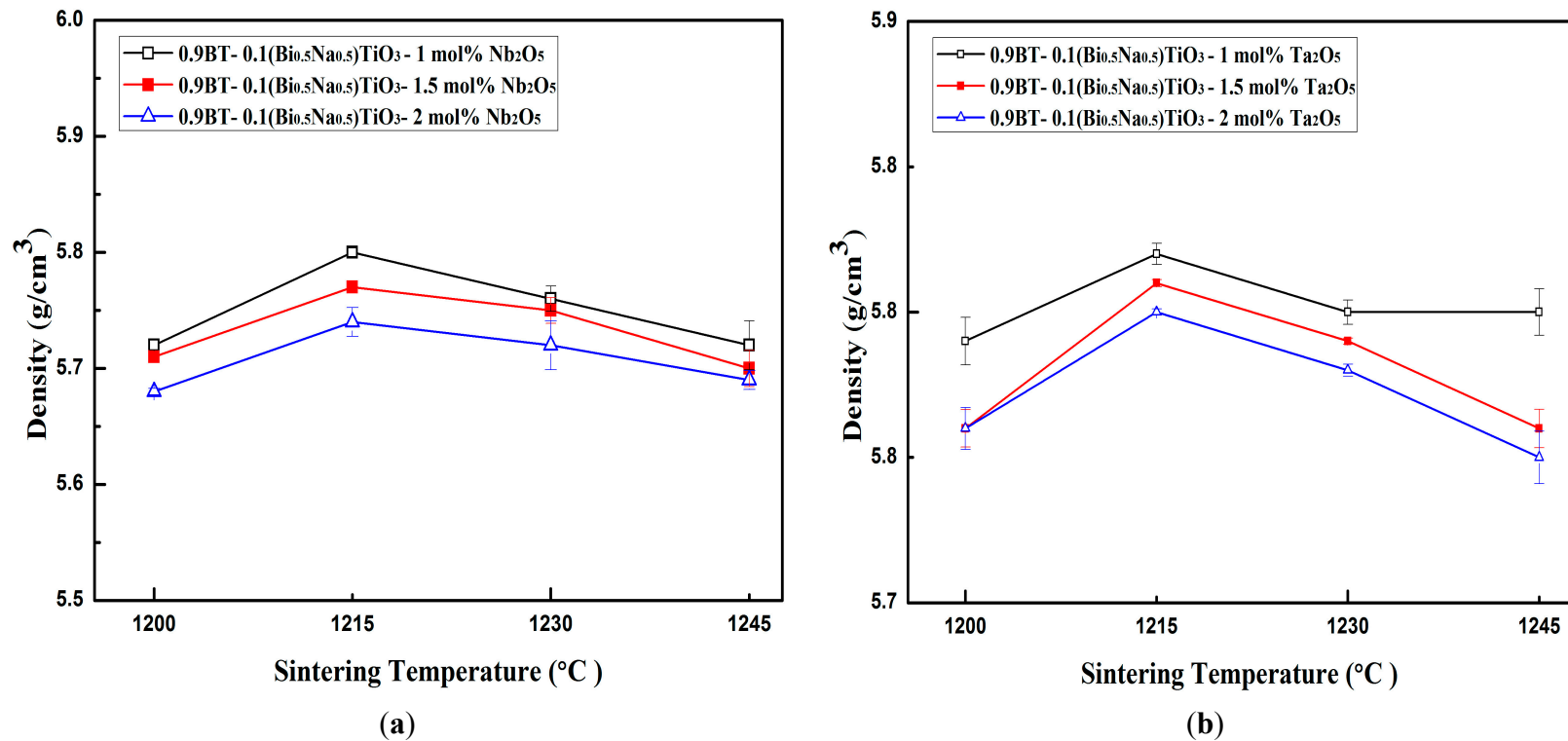


Figure 1. Apparent densities of $0.9\text{BaTiO}_3 - 0.1(\text{Bi}_{0.5}\text{Na}_{0.5})\text{TiO}_3$ ceramics with various amounts of (a) Ta₂O₅ and (b) Nb₂O₅ sintered at different temperatures for 2 h.

Figure 2a shows the XRD patterns of $0.9\text{BaTiO}_3\text{--}0.1(\text{Bi}_{0.5}\text{Na}_{0.5})\text{TiO}_3$ ceramics with various amounts of Ta_2O_5 sintered at $1215\text{ }^\circ\text{C}$. Only a major phase of tetragonal perovskite was found in the XRD patterns. Several small peaks at around 30° and 43° were due to the $\text{Ba}_6\text{Ti}_{17}\text{O}_{40}$ phase, which was also observed in the pure $0.9\text{BaTiO}_3\text{--}0.1(\text{Bi}_{0.5}\text{Na}_{0.5})\text{TiO}_3$ ceramic. The addition of Ta_2O_5 in the host material did not trigger any additional second phase, implying that the Ta^{5+} ions were substituted into the B-sites of the perovskite lattices and the excess Ti^{4+} ions caused the formation of the $\text{Ba}_6\text{Ti}_{17}\text{O}_{40}$ phase. It was also found that the peaks corresponding to the perovskite phase shifted slightly to lower angles because of the ionic radius of Ta^{5+} (VI; 0.64 \AA), which is slightly larger than that of Ti^{4+} (VI; 0.605 \AA). As revealed in Figure 2b, for the $0.9\text{BaTiO}_3\text{--}0.1(\text{Bi}_{0.5}\text{Na}_{0.5})\text{TiO}_3$ ceramics with various amounts of added Nb_2O_5 sintered at $1215\text{ }^\circ\text{C}$, the XRD patterns are quite similar to those of the sintered ceramics with Ta_2O_5 . However, another second-phase $\text{Ba}_6\text{Ti}_{14}\text{Nb}_2\text{O}_{39}$ (orthorhombic phase, Bm21b; JCPDF 38-1431) was observed as the Nb_2O_5 content increased to 2 mol%, in addition to the $\text{Ba}_6\text{Ti}_{17}\text{O}_{40}$ phase. The calculated lattice constants of the sintered ceramics with 2.0 mol% Ta_2O_5 and Nb_2O_5 were $a = 3.981\text{ \AA}$ and $c = 4.068\text{ \AA}$ and $a = 3.981\text{ \AA}$ and $c = 4.031\text{ \AA}$, respectively. The larger variation in the lattice constants of the Ta_2O_5 -doped ceramic than of the Nb_2O_5 -doped ceramic is correlated with the greater solubility of the former dopant in the perovskite structure than the latter. The limited solubility of Nb_2O_5 led to the formation of $\text{Ba}_6\text{Ti}_{14}\text{Nb}_2\text{O}_{39}$ precipitates.

Figure 3 shows the microstructures of the sintered surfaces and fracture surfaces of the pure $0.9\text{BaTiO}_3\text{--}0.1(\text{Bi}_{0.5}\text{Na}_{0.5})\text{TiO}_3$ ceramic and those with added Ta_2O_5 and Nb_2O_5 sintered at $1215\text{ }^\circ\text{C}$. All the microstructures of the sintered surfaces were composed of two types of grains: fine equiaxed grains and some enlarge rod-like grains. EDS analysis identified the former as the perovskite phase $\text{BaTiO}_3\text{--}(\text{Bi}_{0.5}\text{Na}_{0.5})\text{TiO}_3$ and the latter as the $\text{Ba}_6\text{Ti}_{17}\text{O}_{40}$ phase. The microstructures of the fracture surfaces indicated that all fractures were transgranular mode and revealed the presence of very little porosity. Figure 3a,b show the sintered surface and fracture surface of the pure $0.9\text{BaTiO}_3\text{--}0.1(\text{Bi}_{0.5}\text{Na}_{0.5})\text{TiO}_3$ ceramic sintered at $1215\text{ }^\circ\text{C}$, which included fine equiaxed grains with an average grain size of $0.57\text{ }\mu\text{m}$ and rod-like grains with a size of approximately $3.2\text{ }\mu\text{m}$, similar to those reported in the literature [14]. The microstructures of the sintered surfaces and fracture surfaces of the $0.9\text{BaTiO}_3\text{--}0.1(\text{Bi}_{0.5}\text{Na}_{0.5})\text{TiO}_3$ ceramics with 1.0 and 2.0 mol% Ta_2O_5 sintered at $1215\text{ }^\circ\text{C}$ are shown in Figure 3c,d, and in Figure 3e,f, respectively. Compared with the average grain size of the pure $0.9\text{BaTiO}_3\text{--}0.1(\text{Bi}_{0.5}\text{Na}_{0.5})\text{TiO}_3$ ceramic, the average grain size decreased slightly with the addition of Ta_2O_5 , while the number of intergranular pores appeared to increase. The average grain size of $0.9\text{BaTiO}_3\text{--}0.1(\text{Bi}_{0.5}\text{Na}_{0.5})\text{TiO}_3$ with 1.0% and 2.0% Ta_2O_5 was determined to be 0.55 and $0.46\text{ }\mu\text{m}$, respectively. The Ta_2O_5 dopant caused a reduction in the grain boundary mobility, which led to a decrease in grain size and an increase in trapped pores. The microstructures of the sintered surfaces of the $0.9\text{BaTiO}_3\text{--}0.1(\text{Bi}_{0.5}\text{Na}_{0.5})\text{TiO}_3$ ceramics with 1.0 mol% and 2.0 mol% Nb_2O_5 sintered at $1215\text{ }^\circ\text{C}$ are shown in Figure 3g,h, respectively; the equiaxed grains had an average size of 0.51 and $0.50\text{ }\mu\text{m}$, respectively. The Nb_2O_5 -doped ceramics appeared to have greater porosity than the Ta_2O_5 -doped ceramics. According to Figure 3i,j, which present the microstructures of the fracture surfaces, many fine second-phase precipitates of approximately 50 nm in size were distributed in the microstructure, which was determined to be $\text{Ba}_6\text{Ti}_{14}\text{Nb}_2\text{O}_{39}$ based on the XRD results shown in Figure 2b. The fine second-phase precipitates suppressed the grain growth because of the pinning effect, which dragged the grain boundaries during sintering.

Overall, it can be concluded that the solubility of Ta₂O₅ dopant is greater than that of Nb₂O₅ dopant in the 0.9BaTiO₃–0.1(Bi_{0.5}Na_{0.5})TiO₃ ceramic. The addition of Ta₂O₅ resulted in the lattice expansion of 0.9BaTiO₃–0.1(Bi_{0.5}Na_{0.5})TiO₃ ceramic and reduced the grain boundary mobility and thus slightly inhibited the densification. The average grain size slightly decreased and the number of trapped pores increased with increase of Ta₂O₅ content. In addition to the pre-existing Ba₆Ti₁₇O₄₀ phase, the escalation in addition of Nb₂O₅ in 0.9BaTiO₃–0.1(Bi_{0.5}Na_{0.5})TiO₃ ceramic triggered the formation of Ba₆Ti₁₄Nb₂O₃₉ precipitates with increased quantity. The distributed second phase suppressed the sintered density and generated porosity in 0.9BaTiO₃–0.1(Bi_{0.5}Na_{0.5})TiO₃ ceramic.

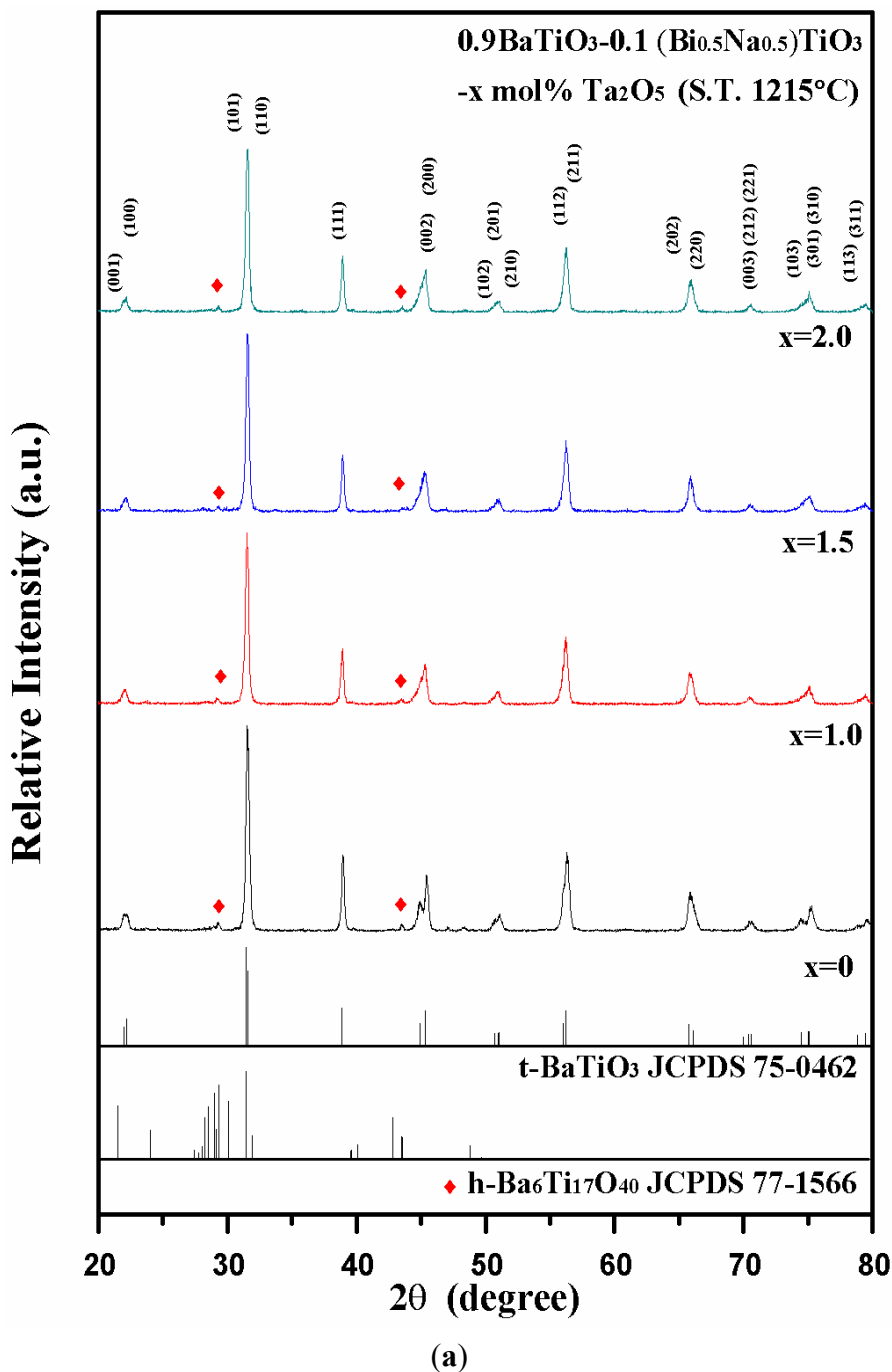


Figure 2. Cont.

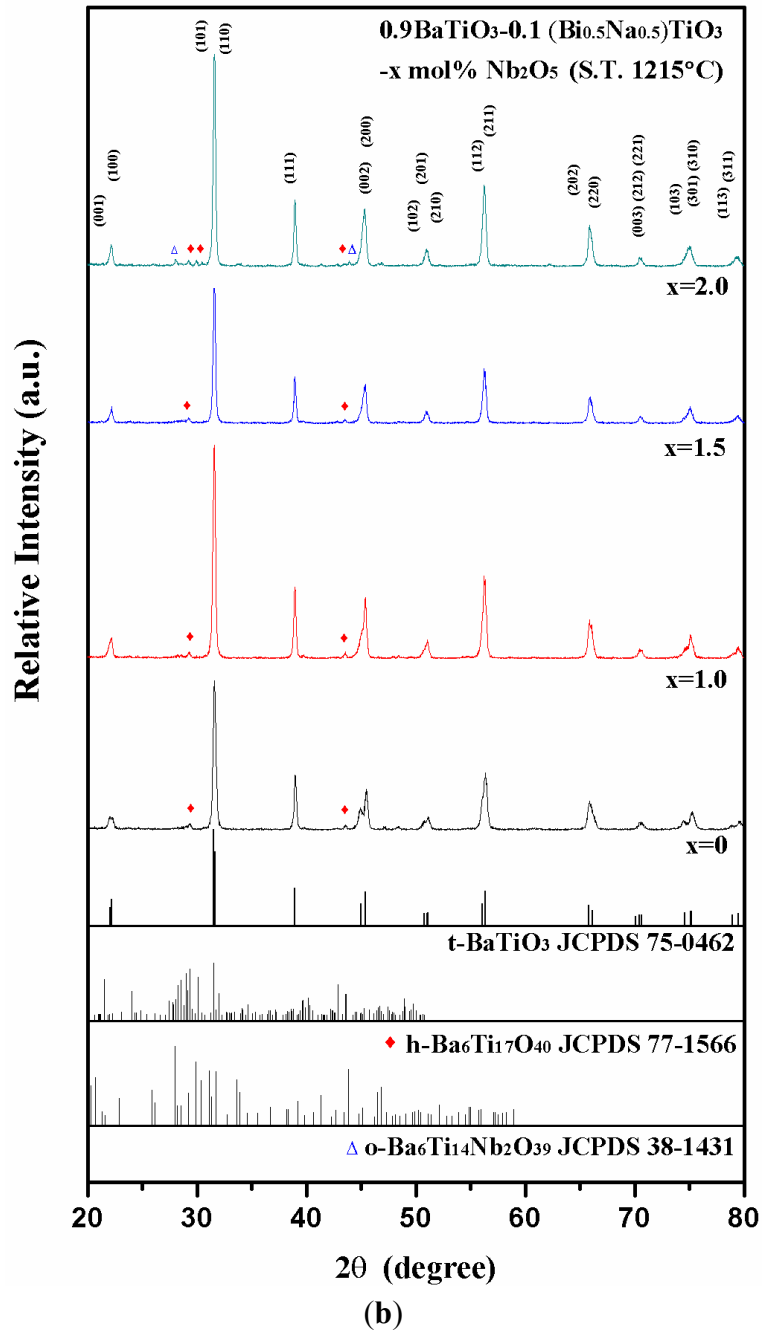


Figure 2. XRD patterns of 0.9BaTiO₃-0.1(Bi_{0.5}Na_{0.5})TiO₃ ceramics with various amounts of (a) Ta₂O₅ and (b) Nb₂O₅ sintered at 1215 °C for 2 h.

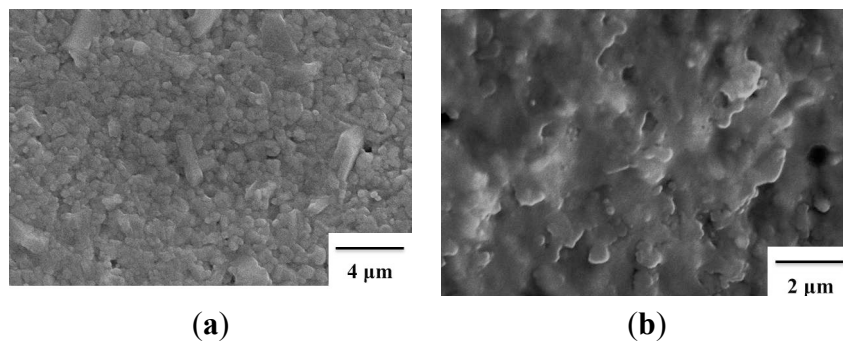


Figure 3. Cont.

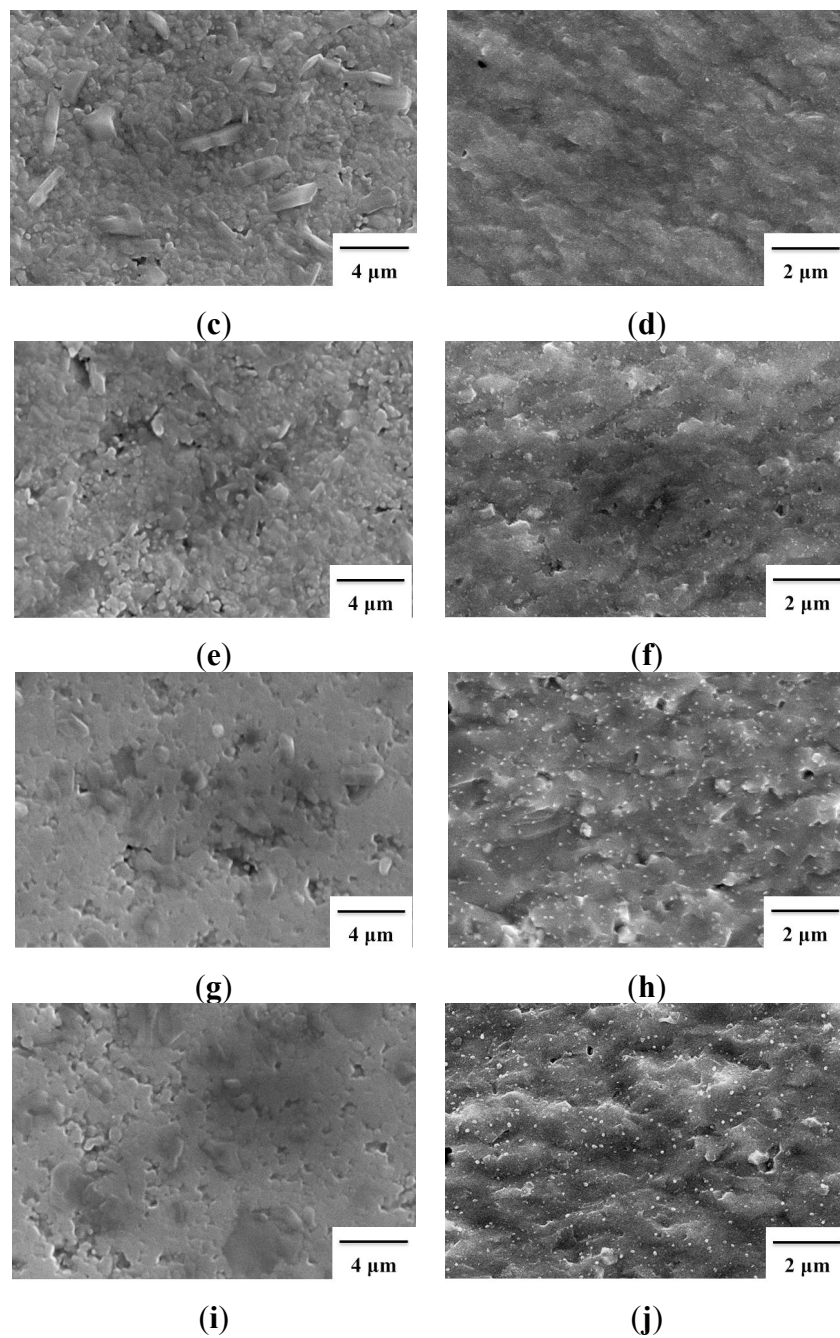
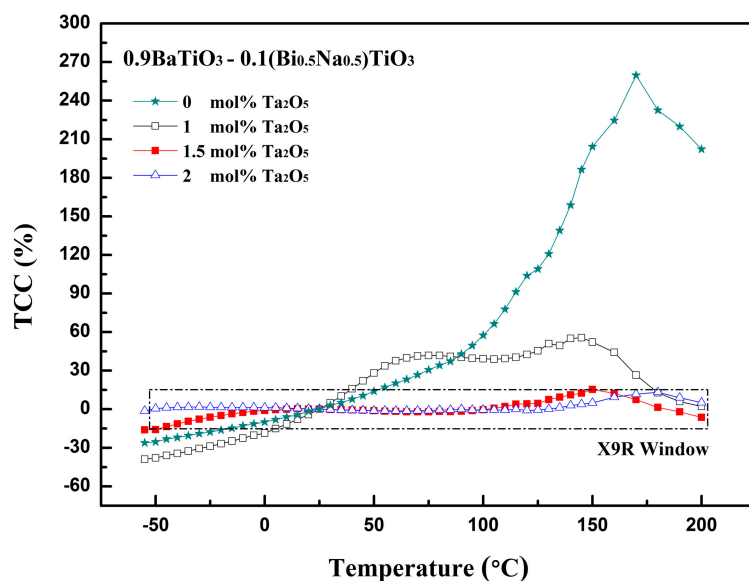


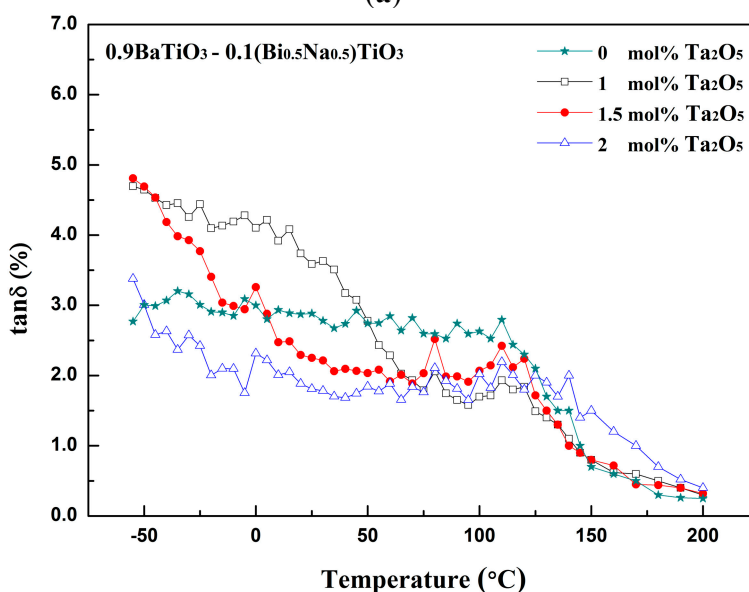
Figure 3. SEM micrographs of the sintered surfaces (a), (c), (e), (g), and (i) and the fractured surfaces (b), (d), (f), (h), and (j) of $0.9\text{BaTiO}_3-0.1(\text{Bi}_{0.5}\text{Na}_{0.5})\text{TiO}_3$ ceramic sintered at $1215\text{ }^\circ\text{C}$ for 2 h. (a) and (b) are pure $0.9\text{BaTiO}_3-0.1(\text{Bi}_{0.5}\text{Na}_{0.5})\text{TiO}_3$ ceramic; (c) and (d) correspond to the ceramic with 1.0 mol% Ta_2O_5 ; (e) and (f) correspond to the ceramic with 2.0 mol% Ta_2O_5 ; (g) and (h) correspond to the ceramic with 1.0 mol% Nb_2O_5 ; and (i) and (j) correspond to the ceramic with 2.0 mol% Nb_2O_5 .

Figures 4 and 5 show the TCCs and dielectric losses *versus* temperature, measured at a frequency of 1 kHz, of $0.9\text{BaTiO}_3-0.1(\text{Bi}_{0.5}\text{Na}_{0.5})\text{TiO}_3$ ceramics with various amounts of added Ta_2O_5 and Nb_2O_5 sintered at $1215\text{ }^\circ\text{C}$, respectively. Some of the dielectric properties, including the Curie point, dielectric constant, and $\tan\delta$ value at $25\text{ }^\circ\text{C}$ and TCCs at both $25\text{ }^\circ\text{C}$ and $200\text{ }^\circ\text{C}$, are also listed in Table 2. The temperature dependence of the $0.9\text{BaTiO}_3-0.1(\text{Bi}_{0.5}\text{Na}_{0.5})\text{TiO}_3$ ceramics became flattened with

an increase in the dopant contents of Ta₂O₅ and Nb₂O₅. The TCC curves near the Curie point were dramatically suppressed, and a broad and diffuse phase transition occurred in all samples, leading to smooth dielectric temperature characteristics over a relatively broad temperature range (−55 to 200 °C). The temperature corresponding to the maximum of the diffuse phase transition (*T_m*) increased with the Ta₂O₅ content, but there was no visible change with an increase in the Nb₂O₅ content. For instance, *T_m* corresponding to the 0.9BaTiO₃–0.1(Bi_{0.5}Na_{0.5})TiO₃ ceramics with 1.0, 1.5, and 2.0 mol% Ta₂O₅ content appeared to be around 145 °C, 150 °C, and 180 °C, respectively, while those with 1.0, 1.5 and 2.0 mol% Nb₂O₅ had a similar *T_m* of approximately 140 °C. It is apparent that the Ta₂O₅ content can effectively elevate the *T_m* of the sintered ceramics.



(a)



(b)

Figure 4. (a) TCCs and (b) dielectric losses *versus* temperature of 0.9BaTiO₃–0.1(Bi_{0.5}Na_{0.5})TiO₃ ceramics with various amounts of Ta₂O₅ sintered at 1215 °C (measured frequency = 1 kHz; heating rate = 2 °C/min; applied voltage = 1 V).

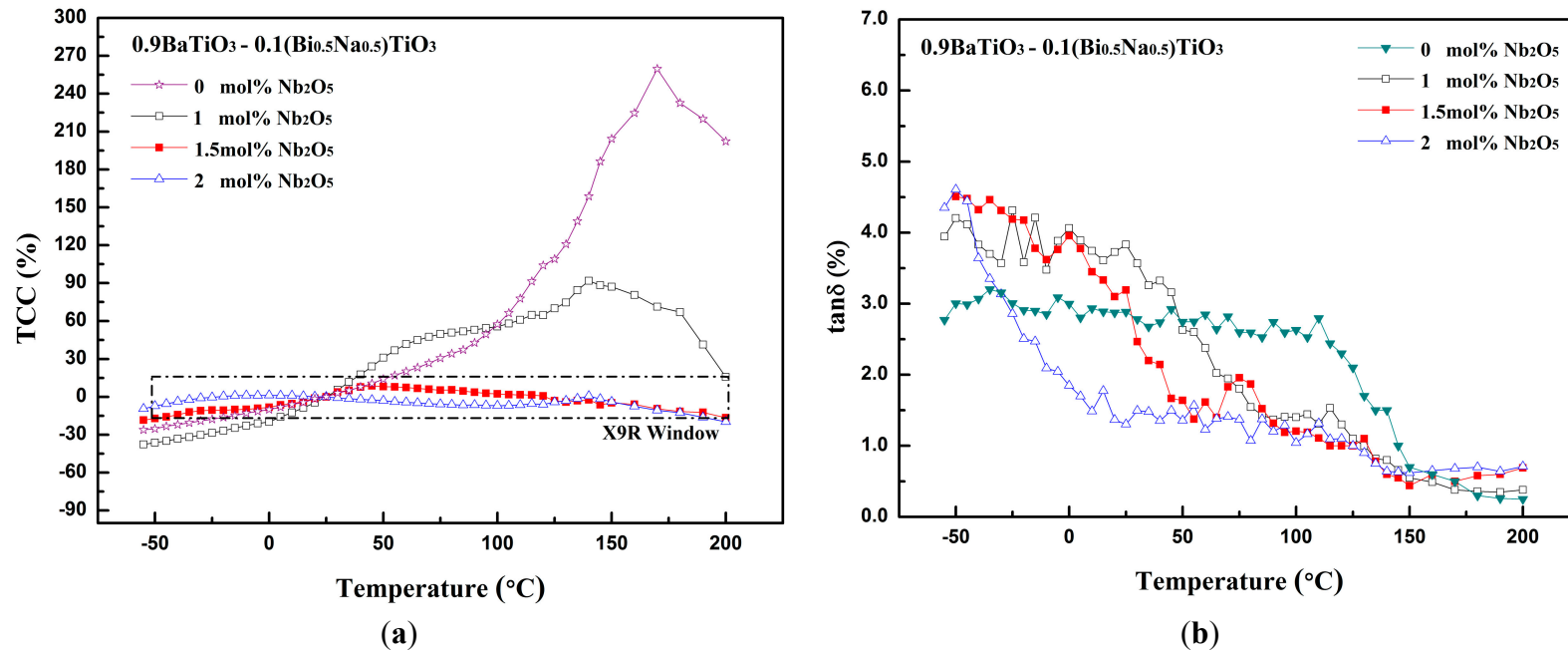


Figure 5. (a) Temperature coefficients of capacitance and (b) dielectric losses *versus* temperature of 0.9BaTiO₃-0.1(Bi_{0.5}Na_{0.5})TiO₃ ceramics with addition of various amounts of Nb₂O₅ sintered at 1215 °C (measured frequency = 1 kHz; heating rate = 2 °C/min; applied voltage = 1 V).

Table 2. Dielectric properties of 0.9BaTiO₃-0.1(Bi_{0.5}Na_{0.5})TiO₃ ceramic with various amounts of Ta₂O₅ and Nb₂O₅ at their maximum sintered densities.

Additives	Sintering Condition (°C/ h)	Sintered Density (g/cm ³)	T _m (°C)	K (25 °C)	tanδ (25 °C)	TCC		Resistivity * (Ω·cm)	
						-55 °C	200 °C	25 °C	200 °C
1.0 mol% Ta ₂ O ₅	1215/2	5.82	145	1788	3.6%	-38.8	2.1	2.6 × 10 ¹²	1.3 × 10 ¹¹
1.5 mol% Ta ₂ O ₅	1215/2	5.81	150	1800	2.3%	-16.1	-6.4	3.5 × 10 ¹²	8.2 × 10 ¹⁰
2.0 mol% Ta ₂ O ₅	1215/2	5.79	180	1386	1.8%	-1.3	5.2	2.8 × 10 ¹²	1.5 × 10 ¹⁰
1.0 mol% Nb ₂ O ₅	1215/2	5.79	140	1471	3.9%	-37.7	15.7	9.0 × 10 ¹²	9.1 × 10 ¹⁰
1.5 mol% Nb ₂ O ₅	1215/2	5.77	140	1790	3.1%	-18.4	-16.5	6.2 × 10 ¹²	5.5 × 10 ¹⁰
2.0 mol% Nb ₂ O ₅	1215/2	5.74	140	1865	1.4%	-9.4	-19.8	7.8 × 10 ¹²	5.1 × 10 ¹⁰

* Resistivity of the samples was measured at a DC voltage of 500 V.

The TCCs of the $0.9\text{BaTiO}_3\text{--}0.1(\text{Bi}_{0.5}\text{Na}_{0.5})\text{TiO}_3$ ceramic with 1.0 mol% Ta_2O_5 at -55 and 200 °C were -38.8% and 2.1% , respectively, which failed to meet the EIA X9R specifications because of the large variation of capacitance between the hot and cold ends (See Figures 4a and 5a). As the Ta_2O_5 dopant content in the sintered ceramic increased, the capacitance variation at both -55 °C and 200 °C became flattened. The TCCs of the sintered ceramics became X9R-qualified with 2.0 mol% Ta_2O_5 . The TCCs at -55 °C and 200 °C for the sintered ceramics with 1.5 and 2.0 mol% Ta_2O_5 were, respectively, -16.1% and -6.4% and -1.3% and 5.2% . The dielectric constant of the $0.9\text{BaTiO}_3\text{--}0.1(\text{Bi}_{0.5}\text{Na}_{0.5})\text{TiO}_3$ ceramic tended to decrease with the Ta_2O_5 content and appeared to be 1788, 1800, and 1386 for 1.0, 1.5 and 2.0 mol% Ta_2O_5 , respectively. However, the dielectric constant increased from 1471 to 1790 and 1865 as the Nb_2O_5 content rose from 1.0 to 1.5 and 2.0 mol%, respectively. Apparently, the dielectric constant increased with the addition of Nb_2O_5 dopant, even though the differences in their microstructures, such as grain size and porosity, seemed to be trivial.

Capacitors for high-temperature applications must possess a low dielectric loss at both room and high temperatures to prevent overheating and failure. As shown in Figures 4b and 5b, all samples revealed a similar trend in their dielectric-loss curves. The dielectric losses of the sintered $0.9\text{BaTiO}_3\text{--}0.1(\text{Bi}_{0.5}\text{Na}_{0.5})\text{TiO}_3$ ceramics with Ta_2O_5 and Nb_2O_5 continued to drop with the measurement temperature. For instance, the dielectric loss of the sintered ceramic with 2.0 mol% Ta_2O_5 was 3.3%, 1.8%, and 1.7% at temperatures of -55 , 25, and 200 °C, respectively. The dielectric loss did not increase at high temperature, unlike that of most ferroelectric ceramics, where the dielectric loss increases because of the increase in ionic mobility or a ferroelectric-paraelectric transition at high temperatures. The dielectric losses of the $0.9\text{BaTiO}_3\text{--}0.1(\text{Bi}_{0.5}\text{Na}_{0.5})\text{TiO}_3$ ceramic were found to decrease significantly with the addition of Ta_2O_5 and Nb_2O_5 . For instance, it decreased from 3.6% to 1.8% and from 3.9% to 1.4% at 25 °C when the Ta_2O_5 and Nb_2O_5 dopant content increased from 1.0 to 2.0 mol%, respectively, which is close to the values for common X7R and X8R ceramics with a similar thickness. The electrical resistivities of the $0.9\text{BaTiO}_3\text{--}0.1(\text{Bi}_{0.5}\text{Na}_{0.5})\text{TiO}_3$ ceramics with added Ta_2O_5 and Nb_2O_5 obtained at 25 °C and 200 °C are also listed in Table 1. All samples appeared to be good insulators, with resistivities ranging from 2.6×10^{12} $\Omega\cdot\text{cm}$ to 9.0×10^{12} $\Omega\cdot\text{cm}$ at 25 °C and from 1.5×10^{10} $\Omega\cdot\text{cm}$ to 1.3×10^{11} $\Omega\cdot\text{cm}$ at 200 °C. There was a decrease of approximately two orders of magnitude in resistivity as the temperature rose from 25 °C to 200 °C.

In this study, it was found that Ta_2O_5 dopant was more efficient to increase the temperature stability of dielectric constant of the $0.9\text{BaTiO}_3\text{--}0.1(\text{Bi}_{0.5}\text{Na}_{0.5})\text{TiO}_3$ ceramic, compared with Nb_2O_5 dopant. Particularly, the host ceramic with 2 mol% Ta_2O_5 dopant had the best composition in terms of dielectric properties. The X9R formulations and their dielectric properties were highly repeatable in this study, which was not the case with the lead-based X9R ceramics reported in the literature [10].

4. Conclusions

$\text{BaTiO}_3\text{--}(\text{Bi}_{0.5}\text{Na}_{0.5})\text{TiO}_3$ ceramics with various amounts of Ta_2O_5 and Nb_2O_5 dopants were explored in the study to compare their high-temperature stability for meeting X9R specifications. Addition of Ta_2O_5 and Nb_2O_5 dopants resulted in a reduction in grain size of the sintered ceramics. The microstructure of the former contained fine equiaxed perovskite grains and some rod-like grains of second-phase $\text{Ba}_6\text{Ti}_{17}\text{O}_{40}$, while that of the latter also included $\text{Ba}_6\text{Ti}_{14}\text{Nb}_2\text{O}_{39}$ precipitates. The best

dielectric properties of the $0.9\text{BaTiO}_3\text{--}0.1(\text{Bi}_{0.5}\text{Na}_{0.5})\text{TiO}_3$ ceramic with 2 mol% Ta_2O_5 dopant sintered at $1215\text{ }^\circ\text{C}$: a dielectric constant of 1386, a $\tan\delta$ of 1.8%, and TCCs of -1.3% and 1.2% and electrical resistivities of 2.8×10^{12} and $1.5 \times 10^{10}\ \Omega\cdot\text{cm}$, respectively, at 25 and $200\text{ }^\circ\text{C}$. The X9R formulations and their dielectric properties were shown to be highly repeatable in this study.

Author Contributions

Sea-Fue Wang and Yung-Fu Hsu conceived and designed the experiments; Yu-Wen Hung and Yi-Xin Liu performed the experiments and analyzed the data; and Sea-Fue Wang wrote the paper.

Conflicts of Interest

The authors declare no conflict of interest.

References

1. Wang, S.F.; Dayton, G.O. Dielectric Properties of Fine-Grain BaTiO_3 Based X7R Dielectric. *J. Am. Ceram. Soc.* **1999**, *82*, 2677–2682.
2. Tang, B.; Zhang, S.R.; Yuan, Y.; Zhou, X.; Liang, Y. Influence of CaZrO_3 on Dielectric properties and Microstructures of BaTiO_3 -Based X8R Ceramics. *Sci. China Ser. E Technol. Sci.* **2008**, *51*, 1451–1456.
3. Tang, B.; Zhang, S.; Zhou, X.; Wang, D.; Yuan, Y. Regression Analysis for Complex Doping of X8R Ceramics Based on Uniform Design. *J. Electron. Mater.* **2007**, *36*, 1383–1388.
4. Sato, S.; Fujikawa, Y.; Nagai, A.; Terada, Y.; Nomura, T. Effect of Rare-Earth Doping on the Temperature-Capacitance Characteristics of MLCCs with Ni electrodes. *J. Ceram. Soc. Jpn.* **2004**, *112*, S481–S485.
5. Yuan, Y.; Zhou, X.H.; Li, B.; Zhang, S.R. Effects of BiNbO_4 and Nb_2O_5 Additions on the Temperature Stability of Modified BaTiO_3 . *Ceram. Silik.* **2010**, *54*, 258–262.
6. Yuan, Y.; Zhou, X.H.; Zhao, C.J.; Li, B.; Zhang, S.R. High-Temperature Capacitor Based on Ca-Doped $\text{Bi}_{0.5}\text{Na}_{0.5}\text{TiO}_3\text{--BaTiO}_3$ Ceramics. *J. Electron. Mater.* **2010**, *39*, 2471–2475.
7. Tang, B.; Zhang, S.R.; Zhou, X.H.; Yuan, Y.; Yang, L.B. Preparation and Modification of High Curie Point BaTiO_3 -Based X9R Ceramics. *J. Electroceram.* **2010**, *5*, 93–97.
8. Li, L.X.; Han, Y.M.; Zhang, P.; Ming, C.; Wei, X. Synthesis and Characterization of BaTiO_3 -Based X9R Ceramics. *J. Mater. Sci.* **2009**, *44*, 5563–5568.
9. Yuan, Y.; Li, E.; Tang, B.; Bo, L.; Zhou, X. Effects of ZnO and CeO_2 Additions on the Microstructure and Dielectric properties of Mn-Modified $(\text{Bi}_{0.5}\text{Na}_{0.5})_{0.88}\text{Ca}_{0.12}\text{TiO}_3$ Ceramics. *J. Mater. Sci. Mater. Electron.* **2012**, *23*, 309–314.
10. Gao, S.; Wu, S.; Zhang, Y.; Yang, H.; Wang, X. Study on the Microstructure and Dielectric properties of X9R Ceramics Based on BaTiO_3 . *Mater. Sci. Eng. B* **2011**, *176*, 68–71.
11. Yuan, Y.; Zhang, S.R.; Zhou, X.H.; Tang, B.; Li, B. High-Temperature Capacitor Materials Based on Modified BaTiO_3 . *J. Electron. Mater.* **2009**, *38*, 706–710.

12. Li, L.; Guo, D.; Xia, W.; Liao, Q.; Han, Y.; Peng, Y. An Ultra-Broad Working Temperature Dielectric Material of BaTiO₃-Based Ceramics with Nd₂O₃ Addition. *Am. Ceram. Soc.* **2012**, *95*, 2107–2109.
13. Zhang, B.; Zhang, B.; Wang, N.; Zhang, J. Low temperature sintering of lead-free BaTiO₃-based X9R ceramics with Bi₂O₃ dopant and assisted by LiF-CaF₂ Flux Agent. *Adv. Mater. Res.* **2014**, *906*, 31–36.
14. Yao, G.; Wang, X.; Wu, Y.; Li, L.T. Nb-Doped 0.9BaTiO₃–0.1(Bi_{0.5}Na_{0.5})TiO₃ Ceramics with Stable Dielectric Properties at High Temperature. *J. Am. Ceram. Soc.* **2012**, *95*, 614–618.
15. Sun, Y.; Liu, H.; Hao, H.; Zhang, L.; Zhang, S. The role of Co in the BaTiO₃–Na_{0.5}Bi_{0.5}TiO₃ based X9R ceramics. *Ceram. Int.* **2015**, *41*, 931–939.
16. Wang, T.; Hao, H.; Liu, M.; Zhou, D.; Yao, Z.; Cao, M.; Liu, H. X9R BaTiO₃-Based Dielectric Ceramics with Multilayer Core–Shell Structure Produced by Polymer-Network Gel Coating Method. *J. Am. Ceram. Soc.* **2015**, *98*, 690–693.
17. Xu, Q.; Huang, D.P.; Chen, M.; Chen, W.; Liu, H.X.; Kim, B.H. Effect of Bismuth excess on Ferroelectric and Piezoelectric Properties of a (Na_{0.5}Bi_{0.5})TiO₃–BaTiO₃ Composition near the Morphotropic Phase Boundary. *J. Alloys Compd.* **2009**, *471*, 310–316.
18. Takeda, H.; Aoto, W.; Shiosaki, T. BaTiO₃–(Bi_{1/2}Na_{1/2})TiO₃ Solid-Solution Semiconducting Ceramics with T_c > 130 °C. *Appl. Phys. Lett.* **2005**, *87*, 102–104.
19. Gao, L.; Huang, Y.; Liu, L.; Lin, T.; Liu, C.; Zhou, F.; Wan, X. Crystal Structure and Properties of BaTiO₃–(Bi_{0.5}Na_{0.5})TiO₃ Ceramic System. *J. Mater. Sci.* **2008**, *43*, 6267–6271.
20. Raengthon, N.; Brown-Shaklee, H.J.; Brennecke, G.L.; Cann, D.P. Dielectric properties of BaTiO₃–Bi(Zn_{1/2}Ti_{1/2})O₃–NaNbO₃ solid solutions. *J. Mater. Sci.* **2013**, *48*, 2245–2250.
21. Chu, B.J.; Chen, D.R.; Li, G.R.; Yin, Q.R. Electrical Properties of Na_{1/2}Bi_{1/2}TiO₃–BaTiO₃ Ceramics. *J. Eur. Ceram. Soc.* **2002**, *22*, 2115–2121.
22. Wang, S.F.; Hsu, Y.F.; Li, J.H.; Lai, Y.C.; Chen, M.H. Dielectric Properties and Microstructures of Non-reducible High-Temperature Stable X9R Ceramics. *J. Eur. Ceram. Soc.* **2013**, *33*, 1793–1799.
23. Hou, J.; Kumar, R.V.; Qub, Y.; Krsmanovic, D. B-site doping effect on electrical properties of Bi₄Ti₃–_{2x}Nb_xTa_xO₁₂ ceramics. *Scr. Mater.* **2009**, *61*, 664–667.
24. Islam, M.F.; Mahub, R.; Mousharraf, A. Effect of Sintering Parameters and Ta₂O₅ Doping on the Microstructure and Dielectric Properties of BaTiO₃ Based Ceramics. *Key Eng. Mater.* **2014**, *608*, 247–252.
25. Kaneko, Y.; Azough, F.; Kida, T.; Ito, K.; Shimada, T. (Ba_{1+x}TiO₃)–(Bi_{0.5}Na_{0.5}TiO₃) Lead-Free, Positive Temperature Coefficient of Resistivity Ceramics: PTC Behavior and Atomic Level Microstructures. *J. Am. Ceram. Soc.* **2012**, *95*, 3928–3934.
26. Datta, K.; Roleder, K.; Thomas, P.A. Enhanced tetragonality in lead-free piezoelectric (1 – x)BaTiO₃–xNa_{1/2}Bi_{1/2}TiO₃ solid solutions where x = 0.05–0.40. *J. Appl. Phys.* **2009**, doi:10.1063/1.3268443.